



# Synthesis, characterization and molecular structures of some tetraosmium carbonyl clusters containing pyridine or phenanthroline type ligands<sup>1</sup>

Ya-Yin Choi, Wing-Tak Wong \*

Department of Chemistry, The University of Hong Kong, Pokfulam Road, Hong Kong, China

Received 3 April 1998

## Abstract

The reactions of activated tetraosmium carbonyl cluster  $[\text{Os}_4(\mu\text{-H})_4(\text{CO})_{11}(\text{NCMe})]$  **1** with monopyridyl ligands give new clusters  $[\text{Os}_4(\mu\text{-H})_4(\text{CO})_{11}(\text{pyp})]$  **3** and  $[\text{Os}_4(\mu\text{-H})_4(\text{CO})_{11}(\text{pya})]$  **4**. Similarly, the reactions of  $[\text{Os}_4(\mu\text{-H})_4(\text{CO})_{10}(\text{NCMe})_2]$  **2** with bipyridyl or phenanthroline type ligands afford  $[\text{Os}_4(\mu\text{-H})_4(\text{CO})_{10}(\text{bpy})]$  **5**,  $[\text{Os}_4(\mu\text{-H})_4(\text{CO})_{10}(\text{dpbpy})]$  **6**,  $[\text{Os}_4(\mu\text{-H})_4(\text{CO})_{10}(\text{phen})]$  **7**,  $[\text{Os}_4(\mu\text{-H})_4(\text{CO})_{10}(\text{dmdpp})]$  **8**, and  $[\text{Os}_4(\mu\text{-H})_4(\text{CO})_{10}(\text{dppz})]$  **9**, which exhibit interesting ring conformations. Treatment of **2** with nitrogen–phosphorus mixed donor ligand gives a novel bridging cluster  $[\text{Os}_4(\mu\text{-H})_4(\text{CO})_{10}(\text{dpppy})]$  **10**. © 1999 Elsevier Science S.A. All rights reserved.

**Keywords:** Osmium; Clusters; Pyridyl ligands; Phenanthroline

## 1. Introduction

Recently, there have been a large number of publications concerning transition metal complexes bearing pyridyl ligands which display the donor–acceptor interactions [1–4]. Apart from their interesting chemical, electrochemical, physical, photophysical and photochemical properties [5–9], their involvement in the construction of supramolecules [10,11] and DNA cleavage species appears to be appealing [12–14]. Such interest has been extended to transition metal clusters, and

numerous trinuclear transition metal clusters containing pyridyl or polypyridyl ligands have been studied extensively [15–19]. With this in mind, we are interested in studying the reactivity of the tetraosmium carbonyl cluster towards some nitrogen-containing ligands such as pyridine or phenanthroline.

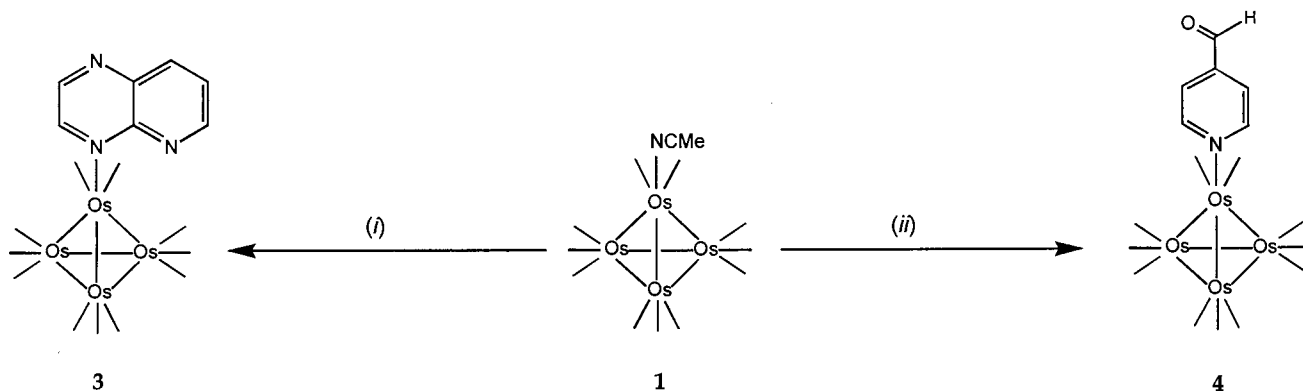
To date, the chemistry of tetraosmium carbonyl clusters containing soft donor atoms such as sulfurs [20,21] and phosphorus [22,23] has been extensively studied. However, the corresponding tetraosmium carbonyl cluster incorporating nitrogen donor ligands is still unknown. It is believed that such complexes will be of fundamental interest for the study of nitrogen functionalized tetraosmium carbonyl clusters.

Apart from these, we would also like to study the reaction of a tetraosmium carbonyl cluster with some heterobidentate ligands, such as 2-(diphenylphosphino)pyridine and 2-(2-thienyl)pyridine. In this report, the synthesis and characterization of a series of tetraosmium carbonyl clusters containing different pyridyl or phenanthroline ligands is described.

*Abbreviations:* pyp, pyrido[2,3-b]pyrazine; pya, 4-pyridinecarboxaldehyde; bpy, 2,2'-bipyridine; dpbpy, 4,4'-diphenyl-2,2'-bipyridine; phen, phenanthroline; dmdpp, 2,9-dimethyl-4,7-diphenyl-1,10-phenanthroline; dppz, dipyrido[3,2-a:2',3'-c]phenazine; dppy, diphenyl-2-pyridylphosphine.

\* Corresponding author. Tel.: +852 28592157; fax: +852 25472933; e-mail: wt Wong@hkucc.hku.hk

<sup>1</sup> Dedicated to Professor Brian F.G. Johnson, on the occasion of his 60th birthday, in recognition of his outstanding contributions to organometallic and inorganic chemistry.



Scheme 1. (i) Pyrido[2,3-b]pyrazine; (ii) 4-pyridinecarboxyaldehyde.

## 2. Results and discussion

### 2.1. Synthesis of the activated tetraosmium carbonyl clusters $[\text{Os}_4(\mu\text{-H})_4(\text{CO})_{11}(\text{NCMe})]$ **1** and $[\text{Os}_4(\mu\text{-H})_4(\text{CO})_{10}(\text{NCMe})_2]$ **2**

The tetraosmium carbonyl cluster  $[\text{Os}_4(\mu\text{-H})_4(\text{CO})_{12}]$  was allowed to react with one or two equivalents of  $\text{Me}_3\text{NO}$  in  $\text{MeCN}$  to give, respectively, the compounds **1** and **2**. A modified procedure to the literature method was employed in the synthesis of cluster **1**. Similar to the previous method, a solution of tetraosmium carbonyl cluster and  $\text{Me}_3\text{NO}$  in a mixture of  $\text{CH}_2\text{Cl}_2$  and  $\text{MeCN}$  (3:2) was stirred for 1 h at room temperature. It was observed that the yield of cluster **1** was increased under gentle warming for another 0.5 h.

### 2.2. Synthesis of $[\text{Os}_4(\mu\text{-H})_4(\text{CO})_{11}(\text{pyp})]$ **3** and $[\text{Os}_4(\mu\text{-H})_4(\text{CO})_{11}(\text{pya})]$ **4**

Cluster **1** and a 2-fold excess of pyrido[2,3-b]pyrazine or 4-pyridinecarboxyaldehyde (Scheme 1) were stirred in warm  $\text{CH}_2\text{Cl}_2$  to give mono-substituted clusters  $[\text{Os}_4(\mu\text{-H})_4(\text{CO})_{11}(\text{pyp})]$  **3** and  $[\text{Os}_4(\mu\text{-H})_4(\text{CO})_{11}(\text{pya})]$  **4**, respectively. Both clusters **3** and **4** have been characterized by conventional solution spectroscopic methods. The spectroscopic data are summarized in Table 9. The fast atom bombardment (FAB) mass spectra of **3** and **4** show a parent peak at 1204 and 1181, respectively. The  $^1\text{H-NMR}$  spectrum of **3** shows resonance signals due to the pyrido[2,3-b]pyrazine group in the range of  $\delta$  7.72–10.07. A broad peak at  $\delta$  –18.2 is also observed which integrates as the four hydrides. Cluster **4** shows two doublets at  $\delta$  7.74 and 8.99 which are attributed to the pyridyl protons, and the signal at  $\delta$  10.11 arises from the aldehyde proton. It was found that all the signals for **3** and **4** appeared to high frequency upon the coordination to the electron deficient metal core when compared with the free ligands.

The molecular geometry of cluster **3** is illustrated in Fig. 1 and selected bond lengths and interbond angles are presented in Table 1. The structure contains a monosubstituted pyrido[2,3-b]pyrazine ligand and the ligand is coordinated to Os(1) through the pyridyl N atom having a  $C_s$  symmetry. The plane containing the ligand and Os(1)–Os(2) bond bisects the  $\text{Os}_4$  metal core. The Os(2)–Os(3) bond [2.814(2) Å] is significantly

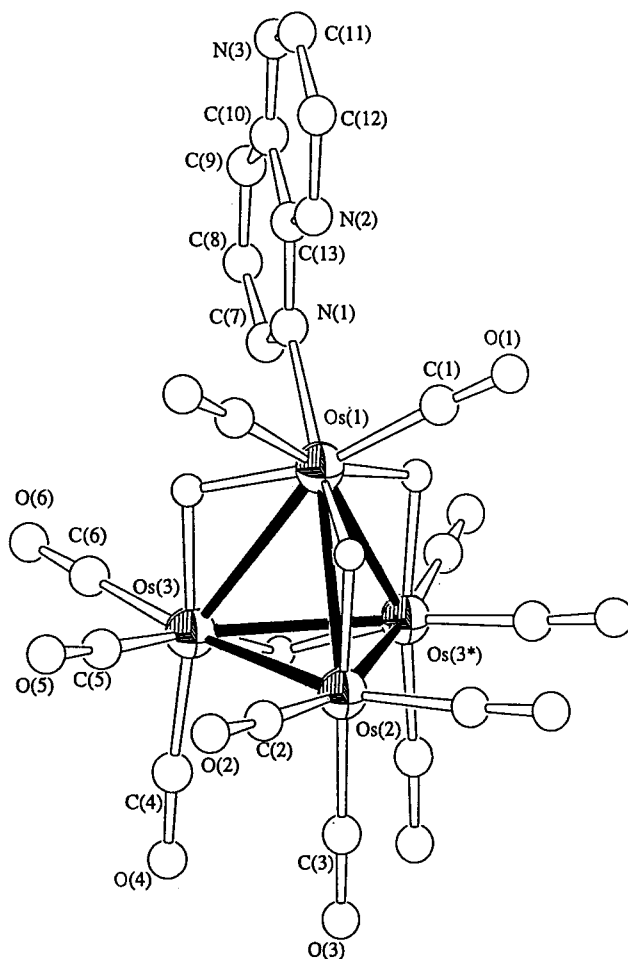


Fig. 1. A perspective drawing of  $[\text{Os}_4(\mu\text{-H})_4(\text{CO})_{11}(\text{pyp})]$  **3**.

Table 1  
Selected bond distances (Å) and angles (°) for cluster **3**

|                    |          |                    |          |
|--------------------|----------|--------------------|----------|
| Os(1)–Os(2)        | 2.930(2) | Os(1)–Os(3)        | 2.988(2) |
| Os(2)–Os(3)        | 2.814(2) | Os(3)–Os(3*)       | 2.943(3) |
| Os(1)–N(1)         | 2.19(3)  |                    |          |
| Os(2)–Os(1)–Os(3)  | 56.48(4) | Os(2)–Os(1)–Os(3*) | 56.78(4) |
| Os(2)–Os(1)–N(1)   | 156.4(6) | Os(3)–Os(1)–Os(3*) | 59.01(4) |
| Os(1)–Os(2)–Os(3)  | 62.66(4) | Os(3)–Os(2)–Os(3*) | 63.06(5) |
| Os(1)–Os(3)–Os(2)  | 60.56(4) | Os(1)–Os(3)–Os(3*) | 60.49(2) |
| Os(2)–Os(3)–Os(3*) | 58.47(3) |                    |          |

shorter than the Os(3)–Os(3\*) bond [2.988(2) Å]. This is consistent with the absence of a bridging hydride along the Os(2)–Os(3) edge in **3**. The same effect was also observed in cluster **4** (Fig. 2), in which the Os(2)–Os(4) and Os(3)–Os(4) [2.806(1) Å and 2.801(1) Å] bonds are substantially shorter than the other Os–Os bonds. Each osmium atom in **3** and **4** [except Os(1) in both cases] is bonded to one axial and two equatorial terminal carbonyl ligands. Details of selected bond parameters for **4** are summarized in Table 2.

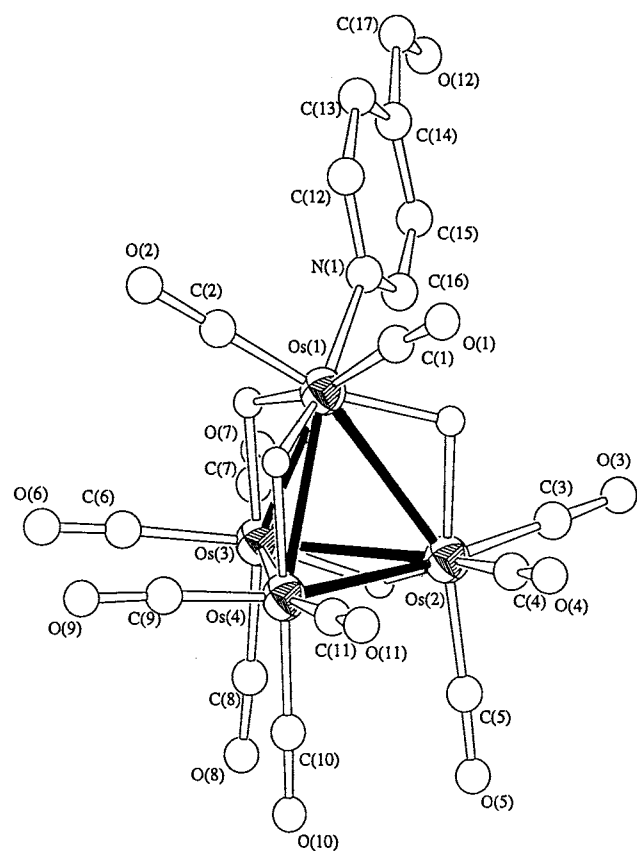


Fig. 2. A perspective drawing of  $[\text{Os}_4(\mu\text{-H})_4(\text{CO})_{11}(\text{pya})]$  **4**.

Table 2  
Selected bond distances (Å) and angles (°) for cluster **4**

|                   |          |                   |          |
|-------------------|----------|-------------------|----------|
| Os(1)–Os(2)       | 2.990(1) | Os(1)–Os(3)       | 3.008(1) |
| Os(1)–Os(4)       | 2.931(1) | Os(2)–Os(3)       | 2.958(1) |
| Os(2)–Os(4)       | 2.806(1) | Os(3)–Os(4)       | 2.801(1) |
| Os(1)–N(1)        | 2.14(2)  |                   |          |
| Os(2)–Os(1)–Os(3) | 59.08(3) | Os(2)–Os(1)–Os(4) | 56.55(3) |
| Os(3)–Os(1)–Os(4) | 56.25(3) | Os(1)–Os(2)–Os(3) | 60.76(3) |
| Os(1)–Os(2)–Os(4) | 60.66(3) | Os(3)–Os(2)–Os(4) | 58.08(3) |
| Os(1)–Os(3)–Os(2) | 60.16(3) | Os(1)–Os(3)–Os(4) | 60.49(3) |
| Os(2)–Os(3)–Os(4) | 58.24(3) | Os(1)–Os(4)–Os(2) | 62.78(3) |
| Os(1)–Os(4)–Os(3) | 63.26(3) | Os(2)–Os(4)–Os(3) | 63.68(3) |

### 2.3. Synthesis of $[\text{Os}_4(\mu\text{-H})_4(\text{CO})_{10}(\text{bpy})]$ **5** and $[\text{Os}_4(\mu\text{-H})_4(\text{CO})_{10}(\text{dpbpy})]$ **6**

A 3-fold excess of 2,2'-bipyridine or 4,4'-diphenyl-2,2'-bipyridine was allowed to react with cluster **2** in  $\text{CH}_2\text{Cl}_2$  giving chelating di-substituted products:  $[\text{Os}_4(\mu\text{-H})_4(\text{CO})_{10}(\text{bpy})]$  **5** and  $[\text{Os}_4(\mu\text{-H})_4(\text{CO})_{10}(\text{dpbpy})]$  **6**, respectively (Scheme 2). Clusters **5** and **6** were fully characterized by various spectroscopic methods. The FAB mass spectra of **5** and **6** show an intense parent peak at 1201 and 1353, respectively. The  $^1\text{H-NMR}$  spectrum of **5** shows a broad peak at  $\delta$  9.28, a doublet at  $\delta$  8.18, and two double doublets at  $\delta$  8.07 and 7.47, which correspond to the proton signals of the bipyridine ligand. The two broad peaks at  $\delta$  –18.1 and –21.0 are due to the four hydrides on the tetraosmium metal core. In the  $^1\text{H-NMR}$  spectrum of **6**, it shows a broad peak at  $\delta$  9.57, two doublets at  $\delta$  8.57 and 7.08, a sharp singlet at  $\delta$  8.08, a double doublet at  $\delta$  7.82 and a triplet 6.93. All of these are attributed to the protons from the organic fragment. Two broad doublets due to the hydrides on the metal core appears at  $\delta$  –18.4 and –20.8. Details of the spectral assignments are presented in Table 9.

The molecular structure of cluster **5** is depicted in Fig. 3 and some important bond lengths and bond angles are shown in Table 3. The structure shows a bidentate 2,2'-bipyridine ligand chelating to Os(1) of the tetrahedral  $\text{Os}_4$  core. The rest of the osmium atoms in the metal core each have three terminal carbonyl ligands. Again, the Os(2)–Os(3) and Os(2)–Os(4) bonds [2.777(1) Å and 2.799(1) Å] are substantially shorter than the other hydride-bridged Os–Os bonds. Similar to **5**, compound **6** consists of a  $\text{Os}_4$  tetrahedron with the 4,4'-diphenyl-2,2'-bipyridine moiety chelated to the Os(1) vertex. The molecular structure of **6** with atom number scheme is shown in Fig. 4 and the selected bond parameters are presented in Table 4. The two pyridine rings of the ligand are nearly coplanar, with the dihedral angle between them being only 1.47°. In the solid state, the phenyl ring [C(26)–C(27)–C(28)–C(29)–C(30)] is nearly coplanar with the two pyridine rings [dihedral angles: 2.0 and 2.9°]; whereas the other

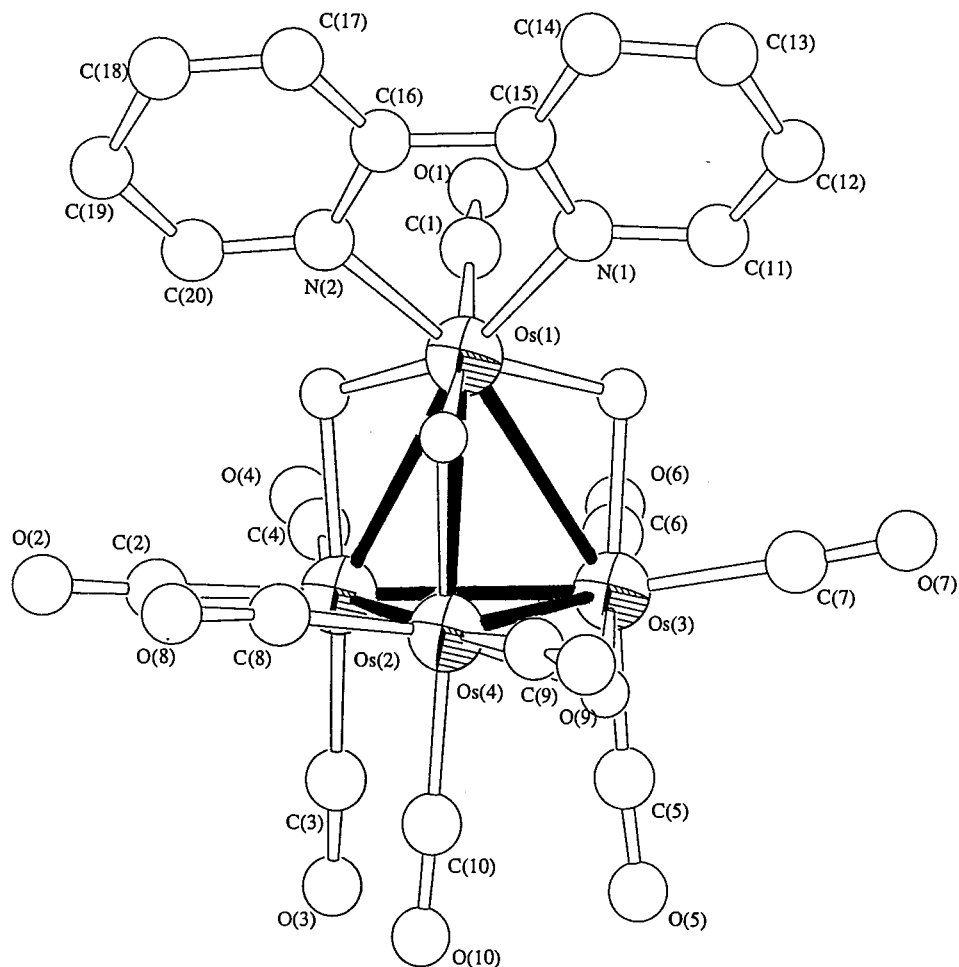


Fig. 3. A perspective drawing of  $[\text{Os}_4(\mu\text{-H})_4(\text{CO})_{10}(\text{bpy})]$  **5**.

phenyl ring [C(14)–C(15)–C(16)–C(17)–C(18)–C(19)] makes a dihedral angle of  $39.1^\circ$  with the pyridine ring [N(1)–C(11)–C(12)–C(13)–C(20)–C(21)].

#### 2.4. Synthesis of $[\text{Os}_4(\mu\text{-H})_4(\text{CO})_{10}(\text{phen})]$ **7**, $[\text{Os}_4(\mu\text{-H})_4(\text{CO})_{10}(\text{dmdpp})]$ **8** and $[\text{H}_4\text{Os}_4(\text{CO})_{10}(\text{dppz})]$ **9**

When cluster **2** and phenanthroline or 2,9-dimethyl-4,7-dimethyl-1,10-phenanthroline or dipyrido[3,2-a:2',3'-

c]phenazine (Scheme 2) were allowed to react in a 1:1 molar ratio in refluxing  $\text{CH}_2\text{Cl}_2$ , disubstituted chelating clusters were obtained:  $[\text{Os}_4(\mu\text{-H})_4(\text{CO})_{10}(\text{phen})]$  **7**,  $[\text{Os}_4(\mu\text{-H})_4(\text{CO})_{10}(\text{dmdpp})]$  **8** and  $[\text{Os}_4(\mu\text{-H})_4(\text{CO})_{10}(\text{dppz})]$  **9**. These three clusters have been studied by conventional spectroscopic methods. The FAB mass spectra of **7**, **8**, and **9** show an intense parent peak at 1224, 1405 and 1326, respectively. The  $^1\text{H-NMR}$  spectrum of **7** shows resonance due to the phenanthroline protons in the range  $\delta$  9.25–7.60. Two broad doublets are observed in the hydride region which correspond to the four hydrides on the tetraosmium core. The  $^1\text{H-NMR}$  spectrum of **8** is much more complicated, and the aromatic protons resonate in the range  $\delta$  7.84–7.48, and the signal of the methyl protons appears at  $\delta$  3.29. The two broad peaks at  $\delta$  –18.4 and  $\delta$  –20.8 are attributed to the four metal hydrides. The proton NMR of **9** shows the signals from the phenanthroline protons as a doublet at  $\delta$  9.84, a broad peak at  $\delta$  9.63, two multiplets at  $\delta$  8.48,  $\delta$  8.09 and a double doublet at  $\delta$  7.95. Details of the assignments are summarized in Table 9.

The molecular geometry of **7**, **8** and **9** is very similar in each case with the ligand being chelated to the vertex

Table 3  
Selected bond distances (Å) and angles ( $^\circ$ ) for cluster **5**

|                   |          |                   |          |
|-------------------|----------|-------------------|----------|
| Os(1)–Os(2)       | 2.931(1) | Os(1)–Os(3)       | 2.940(1) |
| Os(1)–Os(4)       | 3.009(1) | Os(2)–Os(3)       | 2.777(1) |
| Os(2)–Os(4)       | 2.799(1) | Os(3)–Os(4)       | 2.928(1) |
| Os(1)–N(1)        | 2.11(2)  | Os(1)–N(2)        | 2.09(2)  |
| Os(2)–Os(1)–Os(3) | 56.47(3) | Os(2)–Os(1)–Os(4) | 56.20(3) |
| Os(3)–Os(1)–Os(4) | 58.94(3) | Os(1)–Os(2)–Os(3) | 61.94(3) |
| Os(1)–Os(2)–Os(4) | 63.32(3) | Os(3)–Os(2)–Os(4) | 63.34(3) |
| Os(1)–Os(3)–Os(2) | 61.59(3) | Os(1)–Os(3)–Os(4) | 61.71(3) |
| Os(2)–Os(3)–Os(4) | 58.69(3) | Os(1)–Os(4)–Os(2) | 60.48(3) |
| Os(1)–Os(4)–Os(3) | 59.35(3) | Os(2)–Os(4)–Os(3) | 57.98(3) |

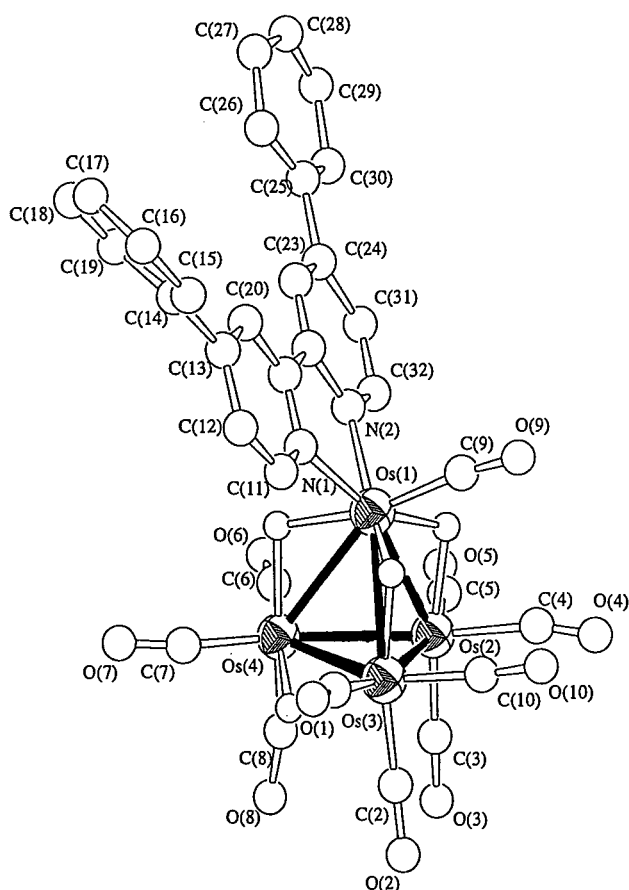


Fig. 4. A perspective drawing of  $[\text{Os}_4(\mu\text{-H})_4(\text{CO})_{10}(\text{dpbpy})]$  **6**.

$[\text{Os}(1)]$  of the tetrahedral tetraosmium core. Perspective drawings of **7**, **8** and **9** are shown in Figs. 5–7, respectively; and selected bonding parameters are summarized in Tables 5–7. Cluster **7** contains two crystallographically independent molecules within the asymmetric unit. The  $\text{Os}(2)\text{--Os}(4)$ ,  $\text{Os}(3)\text{--Os}(4)$  [2.822(2) Å and 2.799(2) Å] bonds are shorter than the other Os–Os bonds; the same being observed in the  $\text{Os}(6)\text{--Os}(7)$  and  $\text{Os}(7)\text{--Os}(8)$  edges. The molecular structure of **8** consists of a tetrahedral  $\text{Os}_4$  core with the ligand attached to the vertex  $[\text{Os}(1)]$ . Each of the other osmium atoms has three carbonyl ligands, one axial and two equatorial.

Table 4  
Selected bond distances (Å) and angles (°) for cluster **6**

|  |          |  |          |
|--|----------|--|----------|
| $\text{Os}(1)\text{--Os}(2)$               | 2.954(2) | $\text{Os}(1)\text{--Os}(3)$               | 2.959(2) |
| $\text{Os}(1)\text{--Os}(4)$               | 3.047(2) | $\text{Os}(2)\text{--Os}(3)$               | 2.793(2) |
| $\text{Os}(2)\text{--Os}(4)$               | 2.819(2) | $\text{Os}(3)\text{--Os}(4)$               | 2.958(2) |
| $\text{Os}(1)\text{--N}(1)$                | 2.11(2)  | $\text{Os}(1)\text{--N}(2)$                | 2.11(2)  |
| $\text{Os}(2)\text{--Os}(1)\text{--Os}(3)$ | 56.36(4) | $\text{Os}(2)\text{--Os}(1)\text{--Os}(4)$ | 56.02(4) |
| $\text{Os}(3)\text{--Os}(1)\text{--Os}(4)$ | 58.99(4) | $\text{Os}(1)\text{--Os}(2)\text{--Os}(3)$ | 61.91(4) |
| $\text{Os}(1)\text{--Os}(2)\text{--Os}(4)$ | 63.65(5) | $\text{Os}(3)\text{--Os}(2)\text{--Os}(4)$ | 63.62(5) |
| $\text{Os}(1)\text{--Os}(3)\text{--Os}(2)$ | 61.73(5) | $\text{Os}(1)\text{--Os}(3)\text{--Os}(4)$ | 61.98(5) |
| $\text{Os}(2)\text{--Os}(3)\text{--Os}(4)$ | 58.64(5) | $\text{Os}(1)\text{--Os}(4)\text{--Os}(2)$ | 60.33(5) |
| $\text{Os}(1)\text{--Os}(4)\text{--Os}(3)$ | 59.03(4) | $\text{Os}(2)\text{--Os}(4)\text{--Os}(3)$ | 57.75(5) |

The  $\text{Os}(2)\text{--Os}(3)$  and  $\text{Os}(2)\text{--Os}(4)$  bonds [2.777(1) Å, 2.8056(9) Å] are shorter than the other Os–Os bonds in the metal core. The phenanthroline part of the ligand is essentially planar and the two phenyl rings [C(25)–C(26)–C(27)–C(28)–C(29)–C(30) and C(31)–C(32)–C(33)–C(34)–C(35)–C(36)] are twisted, making dihedral angles of 62.0 and 70.1°, respectively, with the phenanthroline ring, respectively. These two phenyl rings are nearly perpendicular to each other with a dihedral angle of 89.8°. Cluster **9** shows a very interesting structural feature, where the coplanar ligand affords an inverted Y-shaped geometry with the open end chelated to  $\text{Os}(1)$ . The remaining Os vertices each have three terminal carbonyl ligands. Because of the absence of hydride ligands along the  $\text{Os}(2)\text{--Os}(4)$  and  $\text{Os}(3)\text{--Os}(4)$  edges, these bond lengths are found to be shorter than the other Os–Os bonds within the metal core.

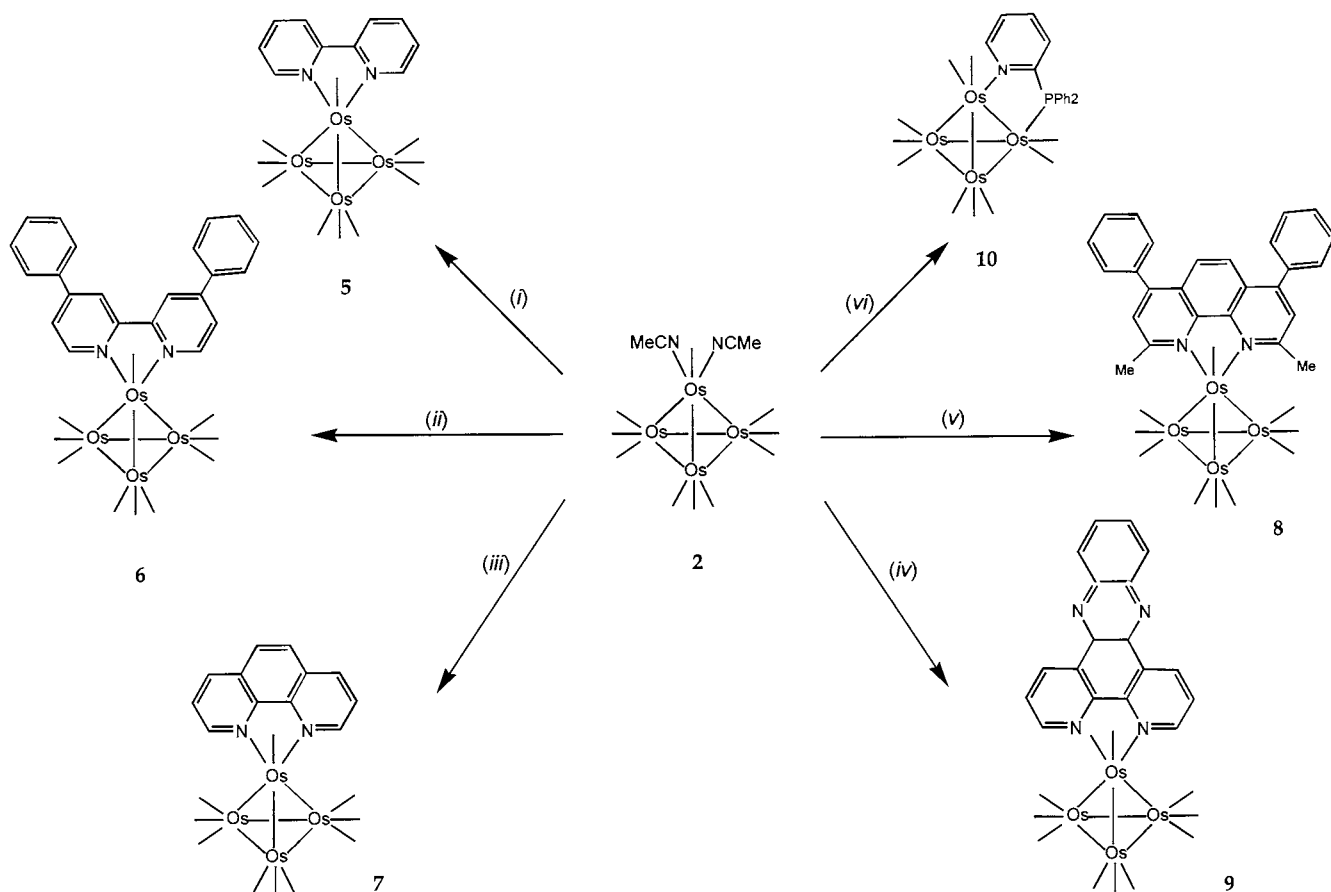
## 2.5. Synthesis of $[\text{Os}_4(\mu\text{-H})_4(\text{CO})_{10}(\text{dppy})]$ **10**

Initial attempts to study the reaction of cluster **2** with a heterobidentate ligand, [2-(2-(thienyl)pyridine)], failed to give any desirable product. However, the reaction of cluster **2** with 2-(diphenylphosphino)pyridine readily yields a bridging product,  $[\text{Os}_4(\mu\text{-H})_4(\text{CO})_{10}(\text{C}_{17}\text{H}_{14}\text{NP})]$  **10** in a manner similar to other heterobimetallic complexes containing 2-(diphenylphosphino)pyridine. The FAB mass spectrum of **10** shows an intense parent peak at 1308. The  $^1\text{H-NMR}$  of **10** shows a doublet at  $\delta$  9.56, two double doublets at  $\delta$  7.25,  $\delta$  6.39 and a doublet at  $\delta$  6.99, which are attributed to the pyridyl protons. The multiplet at  $\delta$  7.54–7.60 is caused by the protons from the  $\text{PPh}_2$  group. The four hydrides on the metal core give two singlets [ $\delta$  –15.97, –24.07] and two doublets [ $\delta$  –17.95 and 19.56]. The  $^{31}\text{P}\{^1\text{H}\}$ -NMR spectrum of **10** shows a singlet due to the phosphine ligand at  $\delta$  –19.16.

The molecular structure of cluster **10** is depicted in Fig. 8; the bonding distances and bond angles are shown in Table 8. Cluster **10** contains a rigid tetrahedral  $\text{Os}_4$  core with a 2-(diphenylphosphino)pyridine bridging across the  $\text{Os}(1)\text{--Os}(2)$  edge. The  $\text{Os}(1)\text{--Os}(2)$  and  $\text{Os}(3)\text{--Os}(4)$  bonds [2.7921(8) Å, 2.806(1) Å] are shorter than the other Os–Os bonds.

## 2.6. Variable temperature $^1\text{H-NMR}$ study

Like the analogs in tetraruthenium carbonyl clusters [24], the proton NMR spectra of clusters **3–9** cannot give a clear assignment to the four hydrides in the tetraosmium core. Clusters **4**, **5**, **6** and **9** were chosen for the variable temperature  $^1\text{H-NMR}$  study from –50 to 25°C. The two broad peaks in cluster **4** resolve to four singlets at  $\delta$  –18.20, –18.73, –24.40 and –25.86. Although the molecular structure of **4** displaces



Scheme 2. (i) 2,2'-Bipyridine; (ii) 4,4'-diphenyl-2,2'-bipyridine; (iii) 1,10-phenanthroline; (iv) diphenyl-2-pyridylphosphine; (v) 2,9-dimethyl-4,7-diphenyl-1,10-phenanthroline; (vi) dipyrido[3,2-a:2',3'-c]phenazine.

an approximate  $C_s$  symmetry and would require a pattern of hydride signals of 1:1:2, it is possible that the deposition of four hydrides is different at low temperature compared to that observed in the solid state. Each of the two hydride broad doublets in clusters **5** and **6** resolves to two sharp singlets at  $\delta$  – 18.10, – 18.83, – 20.87 and – 21.55 for **5**,  $\delta$  – 18.12, – 18.13, – 20.63 and – 21.31 for **6**. Similarly, the two broad doublets for cluster **9** give four singlets at  $\delta$  – 18.05, – 18.79 – 20.68 and – 21.37 (Table 9).

Although it has been shown that the 2-(diphenylphosphino)pyridine-substituted triosmium cluster can undergo fluxional pyridine migrations between metal centers [25], the variable temperature proton NMR study of **10** cannot give any evidence for such fluxional migration in the case of tetraosmium. The Os–P, and Os–N bonds in **10** [2.300(4) Å, and 2.16(1) Å, respectively] are shorter than those in the triosmium case [2.380(4) Å, and 2.22(1) Å]. Thus we believe that the stronger interactions between the ligand and metal core in the tetraosmium complexes prevent such fluxional behavior from occurring.

### 3. Experimental

None of the compounds reported here are particularly air-sensitive. However, all reactions and manipulations were carried out under Ar with the use of standard inert-atmosphere Schlenk techniques. The reactions were monitored by solution IR spectroscopy in the carbonyl stretching region. Solvents were dried by standard procedures and freshly distilled prior to use [26]. The  $^1\text{H-NMR}$  spectra were recorded on a Bruker DPX 300 spectrometer. Variable temperature  $^1\text{H-}$  and  $^{31}\text{P-NMR}$  experiments were carried out in a Bruker DPX 500 spectrometer (85%  $\text{H}_3\text{PO}_4$  for  $^{31}\text{P}$ ). Mass spectra were obtained on a Finnigan MAT 95 mass spectrometer using the FAB technique.

All chemicals, except where stated, were purchased from commercial sources and used as received without any further purification. The starting clusters  $[\text{Os}_4(\mu\text{-H})_4(\text{CO})_{11}(\text{NCMe})]$  **1** and  $[\text{Os}_4(\mu\text{-H})_4(\text{CO})_{10}(\text{NCMe})_2]$  **2** were prepared from  $[\text{Os}_4(\mu\text{-H})_4(\text{CO})_{12}]$  following a slight modification of the literature procedures [27,28]. Dipyrido[3,2-a:2',3'-c]phenazine was prepared by the literature methods [29]. Routine separation of products was carried out in air by thin layer chromatography

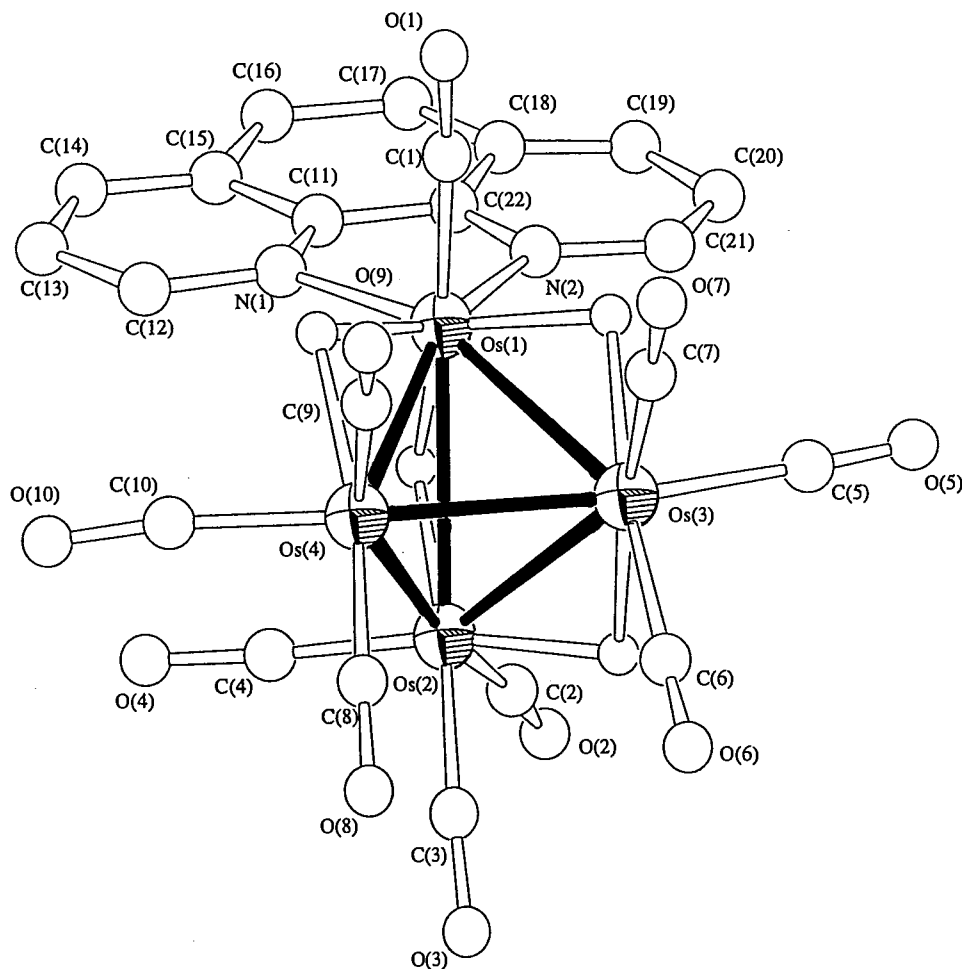


Fig. 5. A perspective drawing of  $[\text{Os}_4(\mu\text{-H})_4(\text{CO})_{10}(\text{phen})]$  **7**.

(TLC) using plates coated with Merck Kieselgel 60 GF<sub>254</sub>.

### 3.1. Preparation of $[\text{Os}_4(\mu\text{-H})_4(\text{CO})_{11}(\text{pyp})]$ **3** and $[\text{Os}_4(\mu\text{-H})_4(\text{CO})_{11}(\text{pya})]$ **4**

Cluster **1** (111 mg, 0.1 mmol) and a 2-fold excess of pyrido[2,3-*b*]pyrazine (52.5 mg, 0.2 mmol) or 4-pyridinecarboxaldehyde (21.4 mg, 0.2 mmol) in  $\text{CH}_2\text{Cl}_2$  (25  $\text{cm}^3$ ) were heated to reflux under an argon atmosphere for 4 h until all starting materials had been consumed, as monitored by TLC. The solvent was removed under reduced pressure and the residue was chromatographed on silica plate with *n*-hexane/dichloromethane (1:1, v/v for **3**; 2:3, v/v for **4**) as eluent. Cluster **3** was isolated as a deep brown solid ( $R_f = 0.6$ ) in 30% yield (41 mg) (Found: C, 17.91; H, 0.57; N, 3.42% Calc. for  $\text{Os}_4\text{C}_{18}\text{H}_9\text{N}_3\text{O}_{11}$ : C, 17.94; H, 0.75; N, 3.49%), and cluster **4** was isolated as an orange solid ( $R_f = 0.5$ ) in 50% yield (60 mg) (Found: C, 17.63;

H, 0.68; N, 1.22% Calc. for  $\text{Os}_4\text{C}_{17}\text{H}_9\text{NO}_{12}$ : C, 17.29; H, 0.76; N, 1.19%).

### 3.2. Preparation of $[\text{Os}_4(\mu\text{-H})_4(\text{CO})_{10}(\text{bpy})]$ **5** and $[\text{Os}_4(\mu\text{-H})_4(\text{CO})_{10}(\text{dpbpy})]$ **6**

Cluster **2** (113 mg, 0.1 mmol) was allowed to react with a 3-fold excess of 2,2'-bipyridine (47 mg, 0.3 mmol), or 4,4'-diphenyl-2,2'-bipyridine (93 mg, 0.3 mmol) in  $\text{CH}_2\text{Cl}_2$  (25  $\text{cm}^3$ ). The reaction mixture was heated to reflux for 4 h under argon atmosphere in each case until no further change was observed by the TLC monitoring. The solvent was evaporated to dryness under vacuum. The residue was purified by TLC using *n*-hexane/dichloromethane (4:6, v/v), as eluent in both cases to give  $[\text{Os}_4(\mu\text{-H})_4(\text{CO})_{10}(\text{bpy})]$  **5** (48 mg, 40% yield) ( $R_f = 0.3$ ) (Found: C, 20.33; H, 0.78; N, 2.42% Calc. for  $\text{Os}_4\text{C}_{20}\text{H}_{12}\text{N}_2\text{O}_{10}$ : C, 19.99; H, 0.99; N, 2.33%), and  $[\text{Os}_4(\mu\text{-H})_4(\text{CO})_{10}(\text{dpbpy})]$  **6** (40 mg, 30% yield) ( $R_f = 0.4$ ), respectively. (Found: C, 27.81; H,

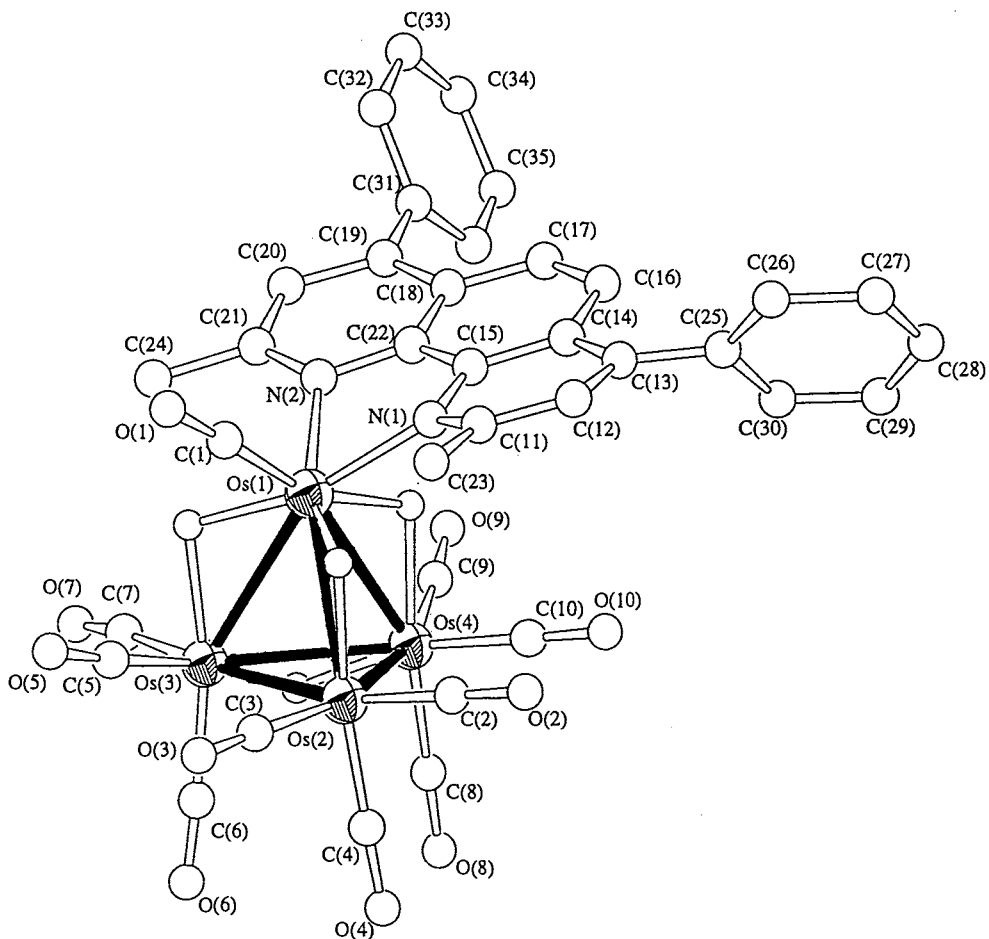


Fig. 6. A perspective drawing of  $[\text{Os}_4(\mu\text{-H})_4(\text{CO})_{10}(\text{dmdpp})]$  **8**.

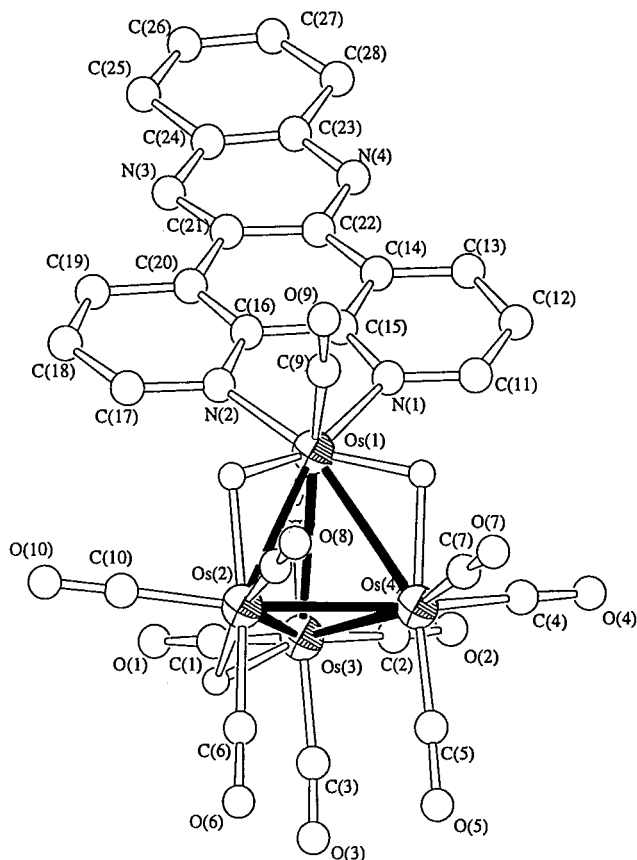
Table 5  
Selected bond distances (Å) and angles (°) for cluster **7**

|                   |          |                   |          |
|-------------------|----------|-------------------|----------|
| Os(1)–Os(2)       | 3.012(1) | Os(1)–Os(3)       | 2.958(2) |
| Os(1)–Os(4)       | 2.938(2) | Os(2)–Os(3)       | 2.956(2) |
| Os(2)–Os(4)       | 2.822(2) | Os(3)–Os(4)       | 2.799(2) |
| Os(5)–Os(6)       | 3.012(1) | Os(5)–Os(7)       | 2.932(2) |
| Os(5)–Os(8)       | 2.954(2) | Os(6)–Os(7)       | 2.821(2) |
| Os(6)–Os(8)       | 2.963(2) | Os(7)–Os(8)       | 2.792(2) |
| Os(1)–N(1)        | 2.12(2)  | Os(1)–N(2)        | 2.11(2)  |
| Os(5)–N(3)        | 2.11(2)  | Os(5)–N(4)        | 2.09(2)  |
| Os(2)–Os(1)–Os(3) | 56.36(4) | Os(2)–Os(1)–Os(4) | 56.61(4) |
| Os(3)–Os(1)–Os(4) | 56.68(4) | Os(1)–Os(2)–Os(3) | 59.42(4) |
| Os(1)–Os(2)–Os(4) | 60.37(4) | Os(3)–Os(2)–Os(4) | 57.88(4) |
| Os(1)–Os(3)–Os(2) | 61.22(4) | Os(1)–Os(3)–Os(4) | 61.29(4) |
| Os(2)–Os(3)–Os(4) | 58.64(4) | Os(1)–Os(4)–Os(2) | 63.02(4) |
| Os(1)–Os(4)–Os(3) | 62.03(4) | Os(2)–Os(4)–Os(3) | 63.47(5) |
| Os(6)–Os(5)–Os(7) | 56.64(4) | Os(6)–Os(5)–Os(8) | 59.55(4) |
| Os(7)–Os(5)–Os(8) | 56.62(4) | Os(5)–Os(6)–Os(7) | 60.25(4) |
| Os(5)–Os(6)–Os(8) | 59.25(4) | Os(7)–Os(6)–Os(8) | 57.65(4) |
| Os(5)–Os(7)–Os(6) | 63.11(4) | Os(5)–Os(7)–Os(8) | 62.09(4) |
| Os(6)–Os(7)–Os(8) | 63.74(4) | Os(5)–Os(8)–Os(6) | 61.20(4) |
| Os(5)–Os(8)–Os(7) | 61.29(4) | Os(6)–Os(8)–Os(7) | 58.61(4) |

1.31; N, 1.98% Calc. for  $\text{Os}_4\text{C}_{32}\text{H}_{20}\text{N}_2\text{O}_{10}$ : C, 28.39; H, 1.48; N, 2.07%

### 3.3. Preparation of $[\text{Os}_4(\mu\text{-H})_4(\text{CO})_{10}(\text{phen})]$ **7**, $[\text{Os}_4(\mu\text{-H})_4(\text{CO})_{10}(\text{dmdpp})]$ **8** and $[\text{Os}_4(\mu\text{-H})_4(\text{CO})_{10}(\text{dppz})]$ **9**

Cluster **2** (113 mg, 0.1 mmol) and 1,10-phenanthroline (18 mg, 0.1 mmol) or 2,9-dimethyl-4,7-diphenyl-1,10-phenanthroline (31 mg 0.1 mmol) or dipyrido[3,2-a:2',3'-c]phenazine (29 mg, 0.1 mmol) were reacted in  $\text{CH}_2\text{Cl}_2$  (25  $\text{cm}^3$ ). The reaction mixture was warmed for 5 h until no change was detected. The solution was concentrated and subjected to preparative TLC, with *n*-hexane/dichloromethane (1:1, v/v) for **8**; (4:6, v/v) for **7** and **9** as eluent. Compound  $[\text{Os}_4(\mu\text{-H})_4(\text{CO})_{10}(\text{phen})]$  **7** was isolated as a red solid in 50% yield (60 mg) ( $R_f = 0.6$ ) (Found: C, 21.67; H, 0.76; N, 2.24% Calc. for  $\text{Os}_4\text{C}_{22}\text{H}_{12}\text{N}_2\text{O}_{10}$ : C, 21.56; H, 0.98; N, 2.29%),  $[\text{Os}_4(\mu\text{-H})_4(\text{CO})_{10}(\text{dmdpp})]$  **8** as a red solid in 20% yield (28 mg) ( $R_f = 0.4$ ), (Found: C, 25.25; H, 1.42;

Fig. 7. A perspective drawing of  $[\text{Os}_4(\mu\text{-H})_4(\text{CO})_{10}(\text{dppz})]$  **9**.Table 6  
Selected bond distances (Å) and angles (°) for cluster **8**

|                   |           |                   |           |
|-------------------|-----------|-------------------|-----------|
| Os(1)–Os(2)       | 2.973(1)  | Os(1)–Os(3)       | 2.9610(9) |
| Os(1)–Os(4)       | 3.0606(9) | Os(2)–Os(3)       | 2.777(1)  |
| Os(2)–Os(4)       | 2.8056(9) | Os(3)–Os(4)       | 2.9627(9) |
| Os(1)–N(1)        | 2.11(1)   | Os(1)–N(2)        | 2.15(1)   |
| Os(2)–Os(1)–Os(3) | 55.81(2)  | Os(2)–Os(1)–Os(4) | 55.40(2)  |
| Os(3)–Os(1)–Os(4) | 58.92(2)  | Os(1)–Os(2)–Os(3) | 61.88(3)  |
| Os(1)–Os(2)–Os(4) | 63.89(2)  | Os(3)–Os(2)–Os(4) | 64.10(2)  |
| Os(1)–Os(3)–Os(2) | 62.31(3)  | Os(1)–Os(3)–Os(4) | 62.22(2)  |
| Os(2)–Os(3)–Os(4) | 58.42(2)  | Os(1)–Os(4)–Os(2) | 60.72(2)  |
| Os(1)–Os(4)–Os(3) | 58.86(2)  | Os(2)–Os(4)–Os(3) | 57.48(2)  |

Table 7  
Selected bond distances (Å) and angles (°) for cluster **9**

|                   |          |                   |          |
|-------------------|----------|-------------------|----------|
| Os(1)–Os(2)       | 2.962(1) | Os(1)–Os(3)       | 3.024(1) |
| Os(1)–Os(4)       | 2.942(1) | Os(2)–Os(3)       | 2.951(1) |
| Os(2)–Os(4)       | 2.793(1) | Os(3)–Os(4)       | 2.819(1) |
| Os(1)–N(1)        | 2.10(1)  | Os(1)–N(2)        | 2.07(2)  |
| Os(2)–Os(1)–Os(3) | 59.06(3) | Os(2)–Os(1)–Os(4) | 56.47(3) |
| Os(3)–Os(1)–Os(4) | 56.36(3) | Os(1)–Os(2)–Os(3) | 61.52(3) |
| Os(1)–Os(2)–Os(4) | 61.41(3) | Os(3)–Os(2)–Os(4) | 58.69(3) |
| Os(1)–Os(3)–Os(2) | 59.42(3) | Os(1)–Os(3)–Os(4) | 60.35(3) |
| Os(2)–Os(3)–Os(4) | 57.85(3) | Os(1)–Os(4)–Os(2) | 62.12(3) |
| Os(1)–Os(4)–Os(3) | 63.29(3) | Os(2)–Os(4)–Os(3) | 63.46(3) |

Table 8  
Selected bond distances (Å) and angles (°) for cluster **10**

|                   |           |                   |           |
|-------------------|-----------|-------------------|-----------|
| Os(1)–Os(2)       | 2.7921(8) | Os(1)–Os(3)       | 2.9883(8) |
| Os(1)–Os(4)       | 2.9153(8) | Os(2)–Os(3)       | 2.9649(9) |
| Os(2)–Os(4)       | 2.9162(9) | Os(3)–Os(4)       | 2.806(1)  |
| Os(1)–P(1)        | 2.300(4)  | Os(2)–N(1)        | 2.16(1)   |
| Os(2)–Os(1)–Os(3) | 61.61(2)  | Os(2)–Os(1)–Os(4) | 61.41(2)  |
| Os(3)–Os(1)–Os(4) | 56.75(2)  | Os(1)–Os(2)–Os(3) | 62.45(2)  |
| Os(1)–Os(2)–Os(4) | 61.38(2)  | Os(3)–Os(2)–Os(4) | 57.00(2)  |
| Os(1)–Os(3)–Os(2) | 55.94(2)  | Os(1)–Os(3)–Os(4) | 60.31(2)  |
| Os(2)–Os(3)–Os(4) | 60.63(2)  | Os(1)–Os(4)–Os(2) | 57.21(2)  |
| Os(1)–Os(4)–Os(3) | 62.93(2)  | Os(2)–Os(4)–Os(3) | 62.37(2)  |

N, 1.82% Calc. for  $\text{Os}_4\text{C}_{36}\text{H}_{24}\text{N}_2\text{O}_{10}$ : C, 25.62; H, 1.71; N, 1.99%) and  $[\text{Os}_4(\mu\text{-H})_4(\text{CO})_{10}(\text{dppz})]$  **9** as a red solid in 50% yield (65 mg) ( $R_f = 0.5$ ). (Found: C, 25.40; H, 0.90; N, 3.94% Calc. for  $\text{Os}_4\text{C}_{28}\text{H}_{14}\text{N}_4\text{O}_{10}$ : C, 25.32; H, 1.06; N, 4.22%)

### 3.4. Preparation of $[\text{Os}_4(\mu\text{-H})_4(\text{CO})_{10}(\text{dpppy})]$ **10**

Cluster **2** (113 mg, 0.1 mmol) and a 2-fold excess of diphenyl-2-pyridylphosphine (56 mg, 0.2 mmol) were mixed and heated to reflux in  $\text{CH}_2\text{Cl}_2$  (30  $\text{cm}^3$ ) under argon atmosphere for 5 h. The solvent was removed under reduced pressure. The residue was subjected to preparative TLC using *n*-hexane/dichloromethane (1:1, v/v) as eluent. An intense orange band containing  $[\text{Os}_4(\mu\text{-H})_4(\text{CO})_{11}(\text{dpppy})]$  **10** was obtained and isolated in 35% yield (45 mg) ( $R_f = 0.5$ ). (Found: C, 24.97; H, 1.29; N, 1.10; P, 2.10% Calc. for  $\text{Os}_4\text{C}_{27}\text{H}_{18}\text{NO}_{10}\text{P}$ : C, 24.77; H, 1.38; N, 1.07; P, 2.36%)

## 4. X-ray crystallography

All pertinent crystallographic data and other experimental details are summarized in Table 10. Intensity data were collected at ambient temperature on a Rigaku AFC7R (**3**, **4**, **8** and **9**) or a MAR research image plate scanner diffractometer (**5**, **6**, **7** and **10**) using  $\text{Mo-K}_\alpha$  radiation ( $\lambda = 0.71073$  Å) with a graphite-crystal monochromator. The  $\omega$ - $2\theta$  scan technique with scan rate of  $16^\circ \text{min}^{-1}$  (in  $\omega$ ) was used for in **3**, **4**, **8** and **9**. For cluster **5**, **6**, **7** and **10**, the  $\omega$  scan technique was employed with 60 3-degree rotation for 5 min per frame. The intensity data were collected for Lorentz and polarization effects. The  $\psi$ -scan method [30] was used for the absorption corrections in **3**, **4**, **8** and **9**. However, an approximation to absorption correction by inter-image scaling was made for other structures. The structures were solved by a combination of direct methods (SIR88) [31] for **5**, (SIR92) [32] for **9** and **10**, (SHELXS86) [33] for **3**, **4**, **6**, **7** and **8**, and difference Fourier techniques. The solutions were refined on  $F$  by full-matrix least-squares analysis with

Table 9  
Summary of spectroscopic data of clusters 3–10

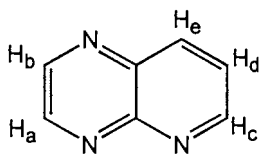
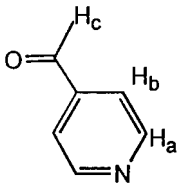
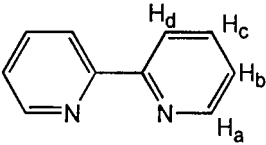
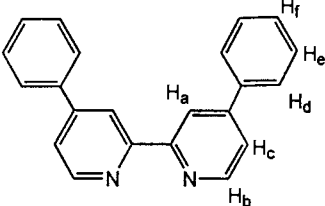
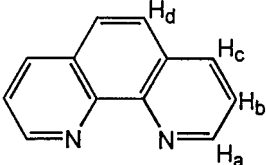
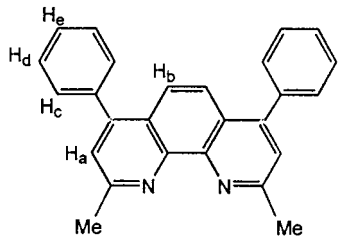
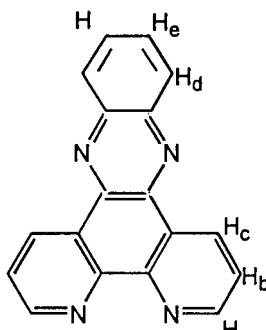
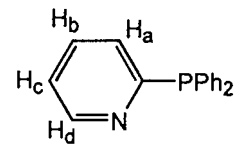
| Cluster | IR( $\nu_{\text{CO}}$ ) <sup>a</sup> (cm <sup>-1</sup> ) | <sup>1</sup> H-NMR <sup>b</sup> ( $\delta$ , $J$ (Hz))  | MS <sup>d</sup>  |
|---------|--|---|--|
| 3       | 2086(s), 2056(vs), 2027(vs), 1999(s), 1981(w)            | 10.07 [1H, d, $J_{\text{ab}}$ 9.5, H <sub>a</sub> ] 8.85 [1H, dd, $J_{\text{cd}}$ 8, H <sub>c</sub> ] 8.63 [1H, m, H <sub>c</sub> ] 8.57 [1H, d, $J_{\text{ab}}$ 9.5, H <sub>b</sub> ] 7.72 [1H, dd, $J_{\text{cd}}$ , $J_{\text{de}}$ 8, 7.8, H <sub>d</sub> ] -18.2 [4H, broad, OsH]  | 1204 (1204)<br>   |
| 4       | 2091(s), 2058(vs), 2030(vs), 1997(s), 1954(w)            | 10.11 [1H, s, H <sub>c</sub> ] 8.99 [2H, d, $J_{\text{ab}}$ 5.5, H <sub>a</sub> ] 7.74 [2H, d, $J_{\text{ab}}$ 5.5, H <sub>b</sub> ] -17.9 [2H, broad, OsH] -24.2 [2H, broad, OsH]  | 1281 (1280)<br>   |
| 5       | 2078(s), 2050(vs), 2018(s), 1996(s), 1971(m)             | 9.28 [1H, broad, H <sub>a</sub> ] 8.18 [2H, d, $J_{\text{cd}}$ 8, H <sub>d</sub> ] 8.07 [2H, dd, $J_{\text{bc}}$ , $J_{\text{cd}}$ 7.5, 8, H <sub>c</sub> ] 7.47 [2H, dd, $J_{\text{ab}}$ , $J_{\text{bc}}$ 6.4, 7.5, H <sub>b</sub> ] -18.1 [2H, broad, OsH] -21.0 [2H, broad, OsH]  | 1201 (1201)<br>   |
| 6       | 2076(s), 2048(vs), 2015(s), 1996(s), 1969(m)             | 9.57 [2H, broad, H <sub>b</sub> ] 8.57 [2H, d, $J_{\text{bc}}$ 8.2, H <sub>c</sub> ] 8.08 [2H, s, H <sub>a</sub> ] 7.82 [2H, dd, $J_{\text{def}}$ 7.7, 7.2, H <sub>e</sub> ] 7.08 [2H, d, $J_{\text{de}}$ 7.7, H <sub>d</sub> ] 6.93 [2H, t, $J_{\text{ef}}$ , $J_{\text{fe}}$ 7.2, H <sub>f</sub> ] -18.4 [2H, bd*, OsH] -20.8 [2H, bd, OsH] | 1353 (1353)<br> |
| 7       | 2076(s), 2047(vs), 2015(s), 1996(s), 1970(m)             | 9.25 [2H, broad, H <sub>a</sub> ] 8.36 [2H, d, $J_{\text{bc}}$ 6, H <sub>c</sub> ] 7.78 [2H, m, H <sub>b</sub> ] 7.60 [2H, m, H <sub>d</sub> ] -18.5 [2H, bd, OsH] -21.2 [2H, bd, OsH]  | 1224 (1225)<br> |
| 8       | 2085(s), 2077(w), 2066(vs), 2046(s), 2018(vs), 1996(s)   | 7.84 [2H, s, H <sub>a</sub> ] 7.72 [2H, m, H <sub>b</sub> ] 7.48–7.60 [10H, m, H <sub>c,d,e</sub> ] 3.29 [6H, m, 2CH <sub>3</sub> ] -18.4 [2H, broad, OsH] -20.8 [2H, broad, OsH]   | 1405 (1405)<br> |

Table 9 (Continued)

| Cluster | IR( $\nu_{\text{CO}}$ ) <sup>a</sup> (cm <sup>-1</sup> ) | <sup>1</sup> H-NMR <sup>b</sup> ( $\delta$ , $J$ (Hz))   | MS <sup>d</sup>   |
|---------|--|--|---|
| 9       | 2077(s), 2048(vs), 2018(s), 1997(s), 1980(m)             | 9.84 [2H, d, $J_{\text{ab}}$ 8, H <sub>a</sub> ] 9.61 [2H, broad, H <sub>c</sub> ] 8.48 [2H, m, H <sub>d</sub> ] 8.09 [2H, m, H <sub>e</sub> ] 7.95 [2H, dd $J_{\text{ab, bc}}$ 8, 5.6, H <sub>b</sub> ] -18.5 [2H, bd, OsH] -21.1 [2H, bd, OsH]   | 1326 (1327)   |
|         |  |  |  |
| 10      | 2087(s), 2050(s), 2029(w), 2004(vs), 1979(m), 1948(w)    | 9.56 [1H, d, $J_{\text{cd}}$ 5.0, H <sub>d</sub> ] 7.4–7.6 [10H, m, C <sub>6</sub> H <sub>5</sub> ] 7.25 [1H, dd, $J_{\text{ab, bc}}$ 6.2, 7.5, H <sub>b</sub> ] 6.99 [1H, d, $J_{\text{ab}}$ 7.5, H <sub>a</sub> ] 6.39 [1H, dd, $J_{\text{bc, cd}}$ 6.2, 5.0, H <sub>c</sub> ] -15.97 [1H, s, OsH] -17.95 [1H, d, $J_{\text{PH}}$ 19.4, OsH] -19.56 [1H, d, $J_{\text{PH}}$ 13.0, OsH] -24.07 [1H, s, OsH] | 1308 (1307)   |
|         |  |  |  |

<sup>a</sup> In CH<sub>2</sub>Cl<sub>2</sub>; <sup>b</sup> in CDCl<sub>3</sub> for 3–9, CD<sub>2</sub>Cl<sub>2</sub> for 10; <sup>c</sup> in CDCl<sub>3</sub>; <sup>d</sup> simulated value in parentheses.

\* bd, broad doublet.

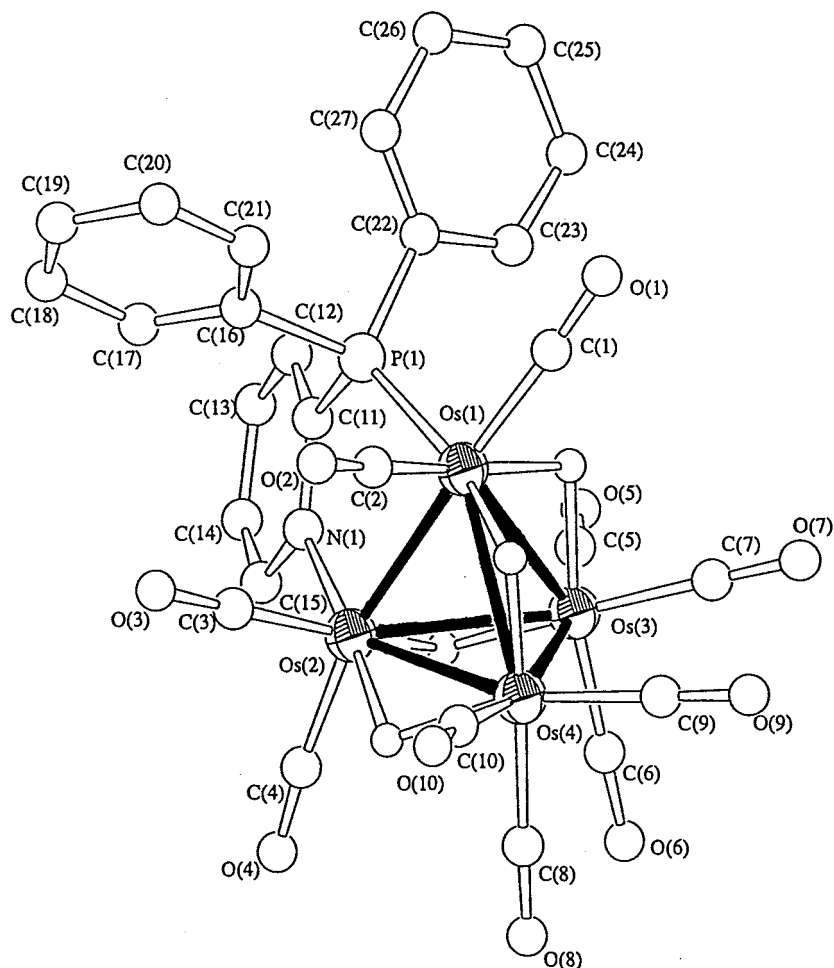


Fig. 8. A perspective drawing of [Os<sub>4</sub>( $\mu$ -H)<sub>4</sub>(CO)<sub>10</sub>(dpppy)] 10.



Os and P atoms varied anisotropically until convergence was reached. The hydrogen atoms of the organic moieties were generated in their ideal positions (C–H 0.95 Å), while hydride atom positions were estimated by potential energy minimizations [34]. All the hydrogen atoms were included in the structure factor calculations but were not refined. All calculations were carried out on a Silicon Graphics workstation using the program package TeXsan [35]. Additional materials available from the Cambridge Crystallographic Data Centre comprise atomic coordinates, thermal displacement parameters and remaining bond distances and angles.

### Acknowledgements

W.T.W. acknowledges financial support from the Hong Kong Research Grants Council and the University of Hong Kong. Y.Y.C. acknowledges the receipt of a postgraduate studentship, the Hung Hing Ying Scholarship and Michael Gale Scholarship administered by the University of Hong Kong and the Hongkong Telecom Foundation. We also thank Dr H.L. Kwong of City University of Hong Kong for his experimental assistance on the preparation of  $[\text{Os}_4(\mu\text{-H})_4(\text{CO})_{12}]$ .

### References

- [1] E.C. Constable, *Prog. Inorg. Chem.* 42 (1994) 67.
- [2] S. Arounaguriri, B.G. Maiya, *Inorg. Chem.* 35 (1996) 4267.
- [3] E.Z. Jandrasics, F.R. Keene, *J. Chem. Soc., Dalton Trans.* (1997) 153.
- [4] A.M.W.C. Thompson, M.C.C. Smailes, J.C. Jeffery, M.D. Ward, *J. Chem. Soc., Dalton Trans.* (1997) 737.
- [5] B. Whittle, S.R. Batten, J.C. Jeffery, L.H. Rees, M.D. Ward, *J. Chem. Soc., Dalton Trans.* (1996) 4249.
- [6] D.A. Bardwell, F. Barigelletti, R.L. Cleary, L. Flamigni, M. Guardigli, J.C. Jeffery, M.D. Ward, *Inorg. Chem.* 34 (1995) 2438.
- [7] J.R. Schoonover, K.C. Gordon, R. Araggzzi, W.H. Woodruff, K.A. Peterson, C.A. Bignozzi, R.B. Dyer, T.J. Meyer, *J. Am. Chem. Soc.* 115 (1993) 10996.
- [8] R.G. Brewer, G.E. Jensen, K.J. Brewer, *Inorg. Chem.* 33 (1994) 124.
- [9] T.S. Akasheh, I. Jibril, A.M. Shraim, *Inorg. Chim. Acta.* 175 (1990) 171.
- [10] W.Y. Wong, W.T. Wong, *J. Chem. Soc., Dalton Trans.* (1995) 1379.
- [11] W.Y. Wong, W.T. Wong, *Inorg. Chim. Acta.* 234 (1995) 5.
- [12] H.H. Thorp, C. Cheng, J.G. Goll, *J. Am. Chem. Soc.* 117 (1995) 2970.
- [13] J.K. Barton, A.T. Danishefsky, J.M. Goldberg, *J. Am. Chem. Soc.* 106 (1984) 2172.
- [14] A.M. Pyle, J.P. Rehmann, R. Meshoyrer, C.V. Kumar, N.J. Turro, J.K. Barton, *J. Am. Chem. Soc.* 111 (1989) 3051.
- [15] W.Y. Wong, S. Chan, W.T. Wong, *J. Chem. Soc., Dalton Trans.* (1995) 1497.
- [16] W.Y. Wong, W.T. Wong, *J. Chem. Soc., Dalton Trans.* (1995) 3995.
- [17] W.Y. Wong, W.T. Wong, *J. Chem. Soc., Dalton Trans.* (1996) 1853.
- [18] E. Kimura, X. Bu, M. Shionoya, S. Wada, S. Maruyama, *Inorg. Chem.* 31 (1992) 4542.
- [19] E.C. Constable, A.M.W.C. Thompson, *J. Chem. Soc., Dalton Trans.* (1995) 1615.
- [20] R.D. Adams, S.B. Falloon, *Organometallics* 14 (1995) 4594.
- [21] Y.Y. Choi, W.T. Wong, unpublished work.
- [22] C.Y. Weil, L. Garlashedi, R. Bau, *J. Organomet. Chem.* 213 (1981) 63.
- [23] Y.Y. Choi, W.T. Wong, *J. Organomet. Chem.* 542 (1996) 121.
- [24] M.R. Churchill, R.A. Lashewycz, J.R. Shapley, S.I. Richter, *Inorg. Chem.* 19 (1980) 1277.
- [25] A.J. Deeming, M.B. Smith, *J. Chem. Soc., Chem. Commun.* (1993) 844.
- [26] D.D. Perrin, W.L.F. Armarego, *Purification of Laboratory Chemicals*, 4th edn, Pergamon, Oxford, 1996.
- [27] H.D. Kaesz, S.A.R. Knox, J.W. Koepke, R.B. Saillant, *J. Chem. Soc., Chem. Commun.* (1971) 477.
- [28] C. Zuccaro, G. Pampaloni, F. Calderazzo, *Inorg. Synth.* 26 (1989) 169.
- [29] J.E. Dickson, L.A. Summers, *Aust. J. Chem.* 23 (1970) 1023.
- [30] A.C.T. North, D.C. Phillips, F.S. Mathews, *Acta Crystallogr. A* 24 (1968) 351.
- [31] M.C. Burla, N. Camalli, G. Cascarano, C. Giacovazzo, G. Polidori, R. Spagna, P. Viterbo, SIR88, *J. Appl. Cryst.* 22 (1989) 389.
- [32] A. Altomare, M.C. Burla, M. Camalli, M. Cascarano, C. Giacovazzo, A. Guagliardi, G. Polidori, SIR92, *J. Appl. Cryst.* 27 (1994) 435.
- [33] G.M. Sheldrick, in: G.M. Sheldrick, C. Kruger, R. Goddard (Eds.), *Crystallographic Computing 3*, Oxford University Press, Oxford, UK, p. 175.
- [34] A.G. Orpen, *J. Chem. Soc., Dalton Trans.* (1980) 2509.
- [35] TeXsan: Crystal Structure Analysis Package, Molecular Structure Corp., Houston, TX, 1985 and 1992.